Front. Chem. Sci. Eng. 2019, 13(1): 120–132
https://doi.org/10.1007/s11705-018-1730-y

RESEARCH ARTICLE

Fabrication of high-capacity cation-exchangers for protein adsorption: Comparison of grafting-from and grafting-to approaches

Ming Zhao[1], Run Liu[1], Jian Luo[3], Yan Sun[1,2], Qinghong Shi (✉)[1,2,3]

1 Department of Biochemical Engineering, School of Chemical Engineering and Technology, Tianjin University, Tianjin 300350, China
2 Key Laboratory of Systems Bioengineering (Ministry of Education), Tianjin University, Tianjin 300072, China
3 State Key Laboratory of Biochemical Engineering, Institute of Process Engineering, Chinese Academy of Sciences, Beijing 100190, China

Abstract In this work, we have synthesized two polymer-grafted cation exchangers: one via the grafting-from approach, in which sulfopropyl methacrylate (SPM) is grafted through atom transfer radical polymerization onto Sepharose FF (the thus resulting exchanger is referred as Sep-*g*-SPM), and another via the grafting-to approach, in which the polymer of SPM is directly coupled onto Sepharose FF (the thus resulting exchanger is called as Sep-*p*SPM). Protein adsorption on these two cation exchangers have been also investigated. At the same ligand density, Sep-*g*-SPM has a larger accessible pore radius and a smaller depth of polymer layer than Sep-*p*SPM, due to the controllable introduction of polymer chains with the regular distribution of the ligand. Therefore, high-capacity adsorption of lysozyme and γ-globulin could be achieved simultaneously in Sep-*g*-SPM with an ionic capacity (IC) of 308 mmol·L^{-1}. However, Sep-*p*SPM has an irregular chain distribution and different architecture of polymer layer, which lead to more serious repulsive interaction to proteins, and thus Sep-*p*SPM has a lower adsorption capacity for γ-globulin than Sep-*g*-SPM with the similar IC. Moreover, the results from protein uptake experiments indicate that the facilitated transport of adsorbed γ-globulin occurs only in Sep-*p*SPM and depends on the architecture of polymer layers. Our research provides a clear clue for the development of high-performance protein chromatography.

Keywords polymer-grafted ionic exchanger, grafting technique, protein adsorption, atom transfer radical polymerization, γ-globulin

Received February 25, 2018; accepted April 1, 2018

E-mail: qhshi@tju.edu.cn

1 Introduction

Polymer-grafted ion exchangers are one of the most striking developments in protein chromatography for biopharmaceutical applications [1–5]. These exchangers always exhibit outstanding adsorption behavior for proteins compared with their non-grafted counterparts [5–9] due to their three-dimensional (3-D) ligand distribution and chain "joggle" arising from flexible polymers grafted on the pore surface of base matrices [8,10]. Nowadays, polymer-grafted ion exchangers can be synthesized via two entirely different techniques: grafting-to and grafting-from approaches [4,11,12]. Sepharose XL® series ion exchangers are the typical representative synthesized via the grafting-to approach, in which flexible dextrans are grafted directly to the pore surface of Sepharose FF matrix before functionalizing with ion or ionizable groups. Recently, Yu et al. attempted to couple charged poly(ethylenimine) (PEI) directly onto Sepharose FF to prepare PEI-grafted anion exchanger [8,13]. They found that charged PEI chains formed an extended 3-D polymer layer over a critical ionic capacity (cIC) of 600 mmol·L^{-1} [8], and thus provided high flexibility and accessibility of the chains for protein binding. In the grafting-from approach, functionalized polymer is grown on the pore surface of matrices by introducing the monomer; Fractogel® EMD series ion exchangers were synthesized by the early version of this approach [14,15]. In 2006, Unsal et al. introduced a new grafting-from approach, surface-initiated atom transfer radical polymerization (ATRP), to synthesize polymer-grafted ion exchangers [12]. This technique was also applied into agarose gel to synthesize high-capacity ion exchangers for protein adsorption by grafting 3-sulfopropyl methacrylate (SPM) monomer onto Sepharose FF matrix [6,11]. For polymer-

grafted ion exchangers to be successful, a deep understanding of polymer role in kinetics and thermodynamics of protein adsorption is critical.

To design high-performance ion exchangers and exploit the potential applications, protein adsorption has extensively been investigated in polymer-grafted ion exchangers since their advent [5–9,14,16–19], revealing many differences from the corresponding non-grafted ion exchangers. Chang and Lenhoff found that tentacle-type Fractogel® EMD·SO_3^- had higher static capacity and affinity for lysozyme adsorption than Toyopearl SP650C with the same base matrix as Fractogel® EMD·SO3$^-$, whereas dextran-grafted SP Spherodex and Bakerbond Carboxy-Sulfone adsorbents both based on silica material showed the opposite [14]. For the above two ion exchangers, the principle difference is grafting techniques. Based on Sepharose matrix, however, Carta [18] and other groups [19] found that dextran-grafted SP Sepharose XL exhibited different performance in protein adsorption comparing with SP Spherodex and had higher adsorption capacity for lysozyme than SP Sepharose FF (non-grafted cation exchangers). Likely, SP Sepharose XL had higher adsorption capacity for antibodies than SP Sepharose FF [20]. By far the highest adsorption capacities (450 mg·mL^{-1} for lysozyme and 313 mg·mL^{-1} for antibody) measured in Sepharose FF matrix were obtained in Sepharose FF grafted with branched SPM polymer via ATRP (grafting-from) approach [11]. However, it had much lower pore diffusivity for proteins than SP Sepharose XL and PEI-grafted Sepharose FF even though the factors of protein size were considered [6,8,11]. The complicated phenomena in polymer-grafted ion exchangers depends most likely on the approaches of surface grafting. To well understand the phenomena in polymer-grafted ion exchangers, therefore, it is essential to provide a detailed investigation about the surface grafting of Sepharose FF for protein adsorption.

In general, the grafting-to approach yields less dense, heterogeneous layers [21]. The grafting-from approach always involves a more complex scheme, and yields a higher grafting density and a highly ordered layer due to less steric effect to a small monomer compared to pre-synthesized polymer applied in the grafting-to approach [21,22]. Therefore, the grafting-to and grafting-from approaches can lead to different architecture and ligand distribution in polymer layers [23–25]. However, to date, very little work on comparison between the grafting-to and grafting-from approaches has been conducted to elucidate the role of polymer layer to the function and the performance of a material for a given application [21,23]. To obtain a meaningful comparison, it is crucial that the molecular characteristics of polymers grafted from and to the surface are identical. It is especially difficult in polymer-grafted ion exchangers to obtain the grafted polymer with identical molecular characteristics via grafting-to and grafting-from approaches.

In this work, two polymer-grafted cation exchangers with identical molecular characteristics of SPM polymer were synthesized via either covalently attached (grafting-to) or atom transfer radical polymerization (grafting-from) approaches to investigate the performance of protein adsorption. To achieve this goal, a new monomer, 2-aminoethyl methacrylate hydrochloride (AEM), was introduced at a very low molar ratio to SPM monomer. AEM was only utilized for the introduction of coupling group in pre-synthesized polymer to Sepharose FF matrix in the grafting-to process, and the influence of AEM on protein adsorption could be ignored. The pre-synthesized polymer was synthesized by applying a free initiator, 2-bromo-2-methylpropionamide (BMPA), in the reaction media via ATRP, and then utilized in the grafting-to process. Hence, the resulting polymers grafted onto Sepharose FF via the grafting-from and grafting-to approaches had the identical molecular characteristics. The physical properties and the adsorption of lysozyme and γ-globulin on the two polymer-grafted cation exchangers were discussed at various ligand densities and salt concentrations. The results are expected to provide new insight about grafting techniques in protein adsorption, which will benefit the development of high-performance ionic exchangers for protein purification.

2 Materials and methods

2.1 Materials

Sepharose FF, SP Sepharose FF and SP Sepharose XL were purchased from GE Healthcare (Uppsala, Sweden). SPM, α-bromoisobutyryl bromide (BIBB), AEM, BMPA, γ-globulin ($>99\%$, M_W ~155000 Da, pI ~6.9), and chicken egg white lysozyme ($>99\%$, MW ~14600 Da, pI ~11.4) were obtained from Sigma-Aldrich (St. Louis, MO). CuBr, CuBr2 and 2,2′-bipyridine (Bpy) were obtained from Dingguo Changsheng Biotech Co. Ltd. (Beijing, China). Triethylamine (TEA) and *N*,*N*-dimethyl formamide (DMF) were received from Guangfu Fine Chemical Research Institute (Tianjin, China). Other reagents were of analytical grade and purchased from local suppliers.

2.2 Fabrication of polymer-grafted cation exchangers

2.2.1 Fabrication of polymer-grafted cation exchangers via ATRP

In this work, polymer-grafted cation exchangers, called as Sep-*g*-SPM, were firstly synthesized via ATRP by grafting SPM monomer onto Sepharose FF according to a modification of the procedure described previously [6,11]. A schematic outline of the synthetic route is shown in Scheme 1. The drained gel (15 g), which was obtained by removing the solvent of Sepharose FF in 20%

ethanol storage solution, was resuspended in 95 mL DMF containing 1.2 mL TEA. The mixture was degassed and cooled in an ice bath under nitrogen, and then a solution of BIBB in DMF (8%, v/v, 12.5 mL) was added dropwise. The acylation reaction was allowed to proceed at 30 °C for 12 h. The resulting bromide-immobilized gel was washed with excess DMF, ethanol and distilled water to remove residual reagents, and is referred to as Sepharose-Br.

In the synthesis of Sep-*g*-SPM cation-exchangers, both Sepharose-Br and BMPA were used as ATRP initiators and SPM was grafted from the pore surface of Sepharose-Br and reaction media. Sepharose-Br was immersed into an Erlenmeyer flask (50 mL) containing $CuBr_2$ (0.05 mmol), Bpy (3.6 mmol), BMPA, and the monomers in an aqueous solution of DMF (67%, v/v, 21 mL). Table 1 lists the amounts of SPM and AEM monomers as well as BMPA used for the synthesis of Sep-*g*-SPM cation exchangers with about 100, 200 and 300 mmol·L^{-1} ligand densities. After the mixture was purged with nitrogen for 30 min, CuBr (1.8 mmol) was added into the flask and then the mixture was purged continuously with nitrogen for 30 min. After the flask was sealed with a rubber stopper, the reaction was carried out at 25 °C and 170 r·min^{-1} for 24 h. The product and supernatant were collected by filtration through a G3 sintered glass filter. After residual copper ion was removed by washing with excess 0.1 mol·L^{-1} EDTA, the collected product was further washed with excess distilled water. This series of the product in Table 1 was

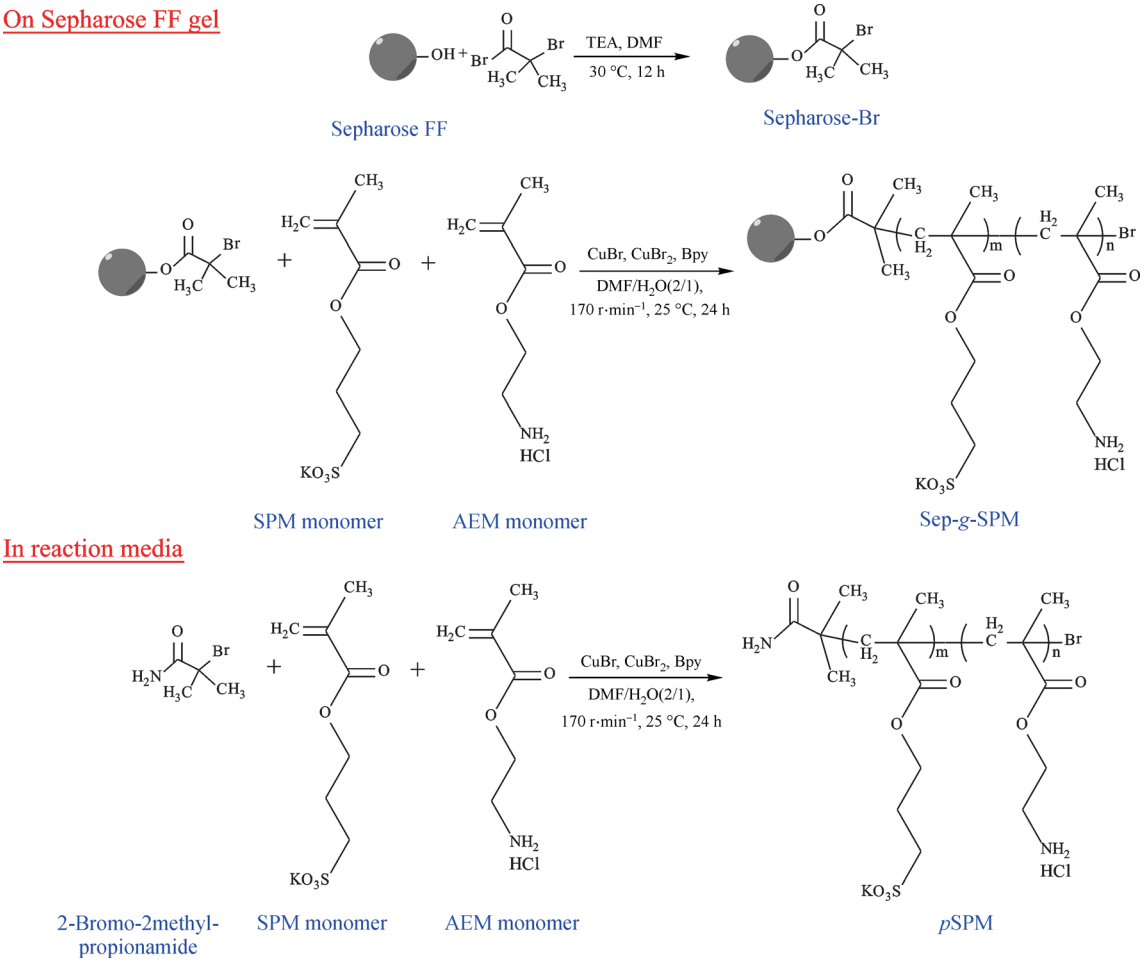

Scheme 1 Preparation of "Sep-*g*-SPM" cation-exchangers and synthetic polymer of SPM (*p*SPM) via ATRP

Table 1 Synthetic information of polymer-grafted cation exchangers and *p*SPM via ATRP

Name	Sepharose-Br/g	SPM/mmol	AEM/mmol	Bpy/mmol	$CuBr_2$/mmol	CuBr/mmol	BMPA/mmol	Solvent/mL
Sep-*g*-SPM300	3	10.0	0.50	3.6	0.05	1.8	0.6	21
Sep-*g*-SPM200	3	6.5	0.33	3.6	0.05	1.8	0.6	21
Sep-*g*-SPM100	3	2.0	0.10	3.6	0.05	1.8	0.6	21
*p*SPM	–	72	3.60	3.6	0.05	1.8	1.2	24

named based on the ligand densities of the Sep-*g*-SPM cation exchangers.

2.2.2 Fabrication of polymer-grafted cation exchangers via grafting-to approach

*p*SPM was synthesized according to the amounts of the monomers and BMPA listed in Table 1 and the procedure described above in the absence of Sepharose-Br. Then Sep-*p*SPM, was prepared by coupling *p*SPM onto Sepharose FF as described by Yu et al. with minor modifications [26]. Briefly, the drained Sepharose FF (10 g) was mixed with a NaOH solution (20 mL, 1 mol·L^{-1}), epichlorohydrin (10 mL) and dimethyl sulfoxide (20 mL), and then activated in an incubator at 25 °C and 170 r·min^{-1} for 2 h. The activated gel was washed with distilled water and drained in a G3 glass filter. Then, the activated Sepharose FF (3 g) was transferred into a flask containing a *p*SPM solution (3 mL), and the slurry was shaken in an incubator at 25 °C and 220 r·min^{-1} for 24 h. Table 2 lists the added amounts of *p*SPM used for the synthesis of Sep-*p*SPM cation exchangers with about 100, 150, 200 and 450 mmol·L^{-1} ligand densities. After that, a NaOH solution (3 mL, 2 mol·L^{-1}) was transferred into the flask and the reaction was carried out at 25 °C and 220 r·min^{-1} for 48 h. The product was collected by filtration through a G3 sintered glass filter and then washed with excess distilled water. This series of the products in Table 2 were named based on ligand densities of Sep-*p*SPM cation exchangers.

Table 2 Synthetic information of polymer-grafted cation exchangers via grafting-to approach

Name	Epoxying resin/g	*p*SPM/(g·mL^{-1})
Sep-*p*SPM100	3.0	0.7–1.0
Sep-*p*SPM150	3.0	1.0–2.0
Sep-*p*SPM200	3.0	2.0–2.5
Sep-*p*SPM450	3.0	3.0–4.0

2.3 Characterization of polymer-grafted cation-exchangers

Fourier-transform infrared (FTIR) spectroscopy was measured on a Shimadzu IRAffinity-1S FTIR spectrometer (Tokyo, Japan) to characterize the chemical structures of Sepharose FF, Sepharose-Br, representative Sep-*g*-SPM and Sep-*p*SPM cation exchangers. Samples were scanned from 4000 to 525 cm^{-1}. The bromide density of Sepharose-Br was analyzed by oxygen flask combustion followed by ion chromatography as described previously [11]. The volume-weighted average diameter of particles (d_p) was measured with a Mastersizer 2000U particle size analyzer from Malvern Instruments Ltd. (Worcestershire, UK). The density of the particles (ρ_p) was measured with a pycnometer (25 mL) at 25 °C [27]. The ionic capacities (ICs) of Sep-*g*-SPM and Sep-*p*SPM cation exchangers were determined by acid-base titration as described by Shi et al. [9]. Inverse size exclusion chromatography (iSEC) was conducted using glucose and dextran probes with molecular weights of 4.32–521 kDa to determine the distribution coefficients (K_D) and accessible pore radius (r_{pore}) of Sepharose FF, SP Sepharose FF, SP Sepharose XL, Sep-*g*-SPM and Sep-*p*SPM cation exchangers as described previously [5,6,8].

2.4 Static adsorption experiments

Adsorption isotherms of lysozyme and γ-globulin on the cation exchangers were carried out by finite batch experiments as described previously with a minor modification [9]. The base buffers were Tris-HCl buffer (pH 8.0, 20 mmol·L^{-1}) for lysozyme adsorption and acetate buffer (pH 4.5, 20 mmol·L^{-1}) for γ-globulin adsorption. In the adsorption buffer, NaCl concentration was adjusted in a range from 0 to 200 mmol·L^{-1}. After the cation exchanger was equilibrated with the adsorption buffer overnight, the drained cation exchanger (50 mg) was mixed with the protein solution (5 mL, 0.5–5 mg·mL^{-1}). The mixture was shaken in an incubator at 170 r·min^{-1} and 25 °C for 24 h. After the reaction, the protein concentration in the supernatant (C) was measured at 280 nm with a PerkinElmer's Lambda 35 UV/VIS spectrophotometer (Shelton, CT) and the adsorption density of the protein (q) was calculated by mass balance. The adsorption isotherms of lysozyme and γ-globulin were described by the Langmuir model

$$q = \frac{q_m C}{K_d + C}, \tag{1}$$

where q_m is the saturated adsorption capacity and K_d is the dissociation constant.

2.5 Lysozyme and γ-globulin uptakes on cation exchangers

Protein uptake were conducted in a three-neck round-bottom flask (200 mL) at 25 °C as described by Yu et al. [26]. After equilibration with the adsorption buffer, a certain amount of the drained cation-exchanger (0.15–1.4 g) was mixed with 100 mL of protein solution (1 mg·mL^{-1} lysozyme and 0.3 mg·mL^{-1} γ-globulin respectively prepared in the corresponding adsorption buffers) to start the experiment at an agitation speed of 280 r·min^{-1}. The real-time liquid phase concentration of proteins in the suspension was measured at 280 nm with a UV-900 detector (GE Healthcare, Uppsala, Sweden) by circulating the solution with P-950 pump (GE Healthcare, Uppsala, Sweden) through a 2.0 μm stainless steel filter at a flow rate of 20 mL·min^{-1}. The effective pore diffusivity of a protein (D_e) was calculated by fitting uptake data to the

pore diffusion model expressed by the following equation:

$$\varepsilon_p \frac{\partial C_p}{\partial t} + \frac{\partial q}{\partial t} = \frac{D_e}{r^2}\frac{\partial}{\partial r}\left(r^2 \frac{\partial C_p}{\partial r}\right), \quad (2)$$

where C_p is the protein concentration in pores and r is the distance in radial direction. For a well-mixed vessel, ignoring the external mass transfer resistance [28], the mass transfer of protein from bulk liquid phase to the surface of solid particles is:

$$\frac{dC}{dt} = \frac{3FD_e}{R}\left(\frac{\partial C_p}{\partial r}\right)_{r=R}, \quad (3)$$

where F is the solid-liquid phase volume ratio, R is the adsorbent radius and C is the bulk liquid phase concentration of protein. The initial and boundary conditions for Eqs. (2) and (3) are

$$\text{initial condition}: t = 0,\ q = 0,\ C_p = 0,\ C = C_0, \quad (4a)$$

$$\text{boundary conditions}: r = R,\ C_p = C, \quad (4b)$$

$$r = 0,\ \frac{\partial C_p}{\partial r} = 0. \quad (4c)$$

The pore diffusion model (Eqs. (2–4)) was solved numerically by the orthogonal collocation method to predict the change of liquid-phase concentration with contact time [11,28]. The experimental data were fitted by MATLAB to obtain D_e values under different conditions.

2.6 Dynamic binding capacity of the cation exchangers

Dynamic binding capacities (DBCs) for lysozyme and γ-globulin of representative Sep-*g*-SPM300 and Sep-*p*SPM450 cation exchangers were measured at room temperature (~25 °C) in a Tricorn 5/50 column connected to an ÄKTA Start chromatography system (GE Healthcare, Uppsala, Sweden). The adsorption buffers were the same as those in static adsorption experiments. After the column was equilibrated with the adsorption buffer, a protein solution (2.0 mg·mL^{-1}) prepared in the adsorption buffer was loaded at 1.0 mL·min^{-1} (300 cm·h^{-1}) for lysozyme and 0.5 mL·min^{-1} (150 cm·h^{-1}) for γ-globulin, and the protein concentration in the effluent was recorded at 280 nm. When the effluent concentration reached 10% of the initial protein concentration, the loading of protein solution was stopped, and a sodium chloride solution (1.0 mol·L^{-1}) was applied to elute the adsorbed protein. Under the non-retained condition, the eluent volume at 10% breakthrough (V_0) was 0.35 mL. DBC is calculated using the following equation

$$\text{DBC} = \frac{C_0(V_{10} - V_0)}{V_B}, \quad (5)$$

where C_0 and V_{10} are the initial protein concentration and loading volume at 10% breakthrough, respectively, and V_B is the column volume.

3 Results and discussion

3.1 Properties of poly(SPM)-grafted cation-exchangers

In this work, three Sep-*g*-SPM cation-exchangers with a bromide density of 5.82 μmol·g^{-1} and four Sep-*p*SPM cation-exchangers were synthesized to investigate the role of grafting techniques on the performance of protein adsorption. As listed in Table 3, all of Sep-*g*-SPM and Sep-*p*SPM cation exchangers have similar d_p and ρ_p values to Sepharose FF, SP Sepharose FF and SP Sepharose XL, indicating that there is no change in the framework of the matrix during polymer grafting. The representative FTIR spectra of Sepharose FF, Sepharose-Br, Sep-*g*-SPM300 and Sep-*p*SPM450 are shown in Fig. 1. Compared with Sepharose FF (Fig. 1(A)), Sepharose-Br (Fig. 1(B)) has the characteristic peak of the carbonyl stretching group at

Table 3 Physical properties of commercial and polymer-grafted cation-exchangers

Name	IC/(mmol·L^{-1})	d_p/μm	ρ_p[b)]/(g·mL^{-1})	C_{NaCl} = 50 mmol·L^{-1}		C_{NaCl} = 200 mmol·L^{-1}	
				r_{pore}/nm	Layer depth/nm	r_{pore}/nm	Layer depth/nm
Sepharose FF	0.0	90±2	1.013	18.7±0.6	–	18.8±0.5	–
SP Sepharose FF[a)]	180–250	90	1.028	17.1±0.7	1.6	17.3±0.6	1.5
SP Sepharose XL	288±2	108±2	1.081	8.3±0.6	10.4	8.8±0.5	10.0
Sep-*g*-SPM100	108±1	91±2	1.030	17.4±0.5	1.3	17.7±0.4	1.1
Sep-*g*-SPM200	204±3	92±2	1.066	15.7±1.1	3.0	16.5±0.9	2.3
Sep-*g*-SPM300	308±2	94±2	1.074	9.6±0.4	9.1	10.3±0.4	8.5
Sep-*p*SPM100	105±1	91±2	1.028	12.5±1.1	6.2	13.3±0.9	5.5
Sep-*p*SPM150	150±4	92±2	1.023	12.4±1.1	6.3	13.2±0.9	5.6
Sep-*p*SPM200	210±5	94±2	1.024	8.8±0.5	9.8	9.5±0.5	9.3
Sep-*p*SPM450	455±6	108±2	1.031	7.7±0.8	10.9	8.4±0.6	10.4

a) Data from DePhillips and Lenhoff [29]; b) all the standard derivatives of ρ_p were 0.001

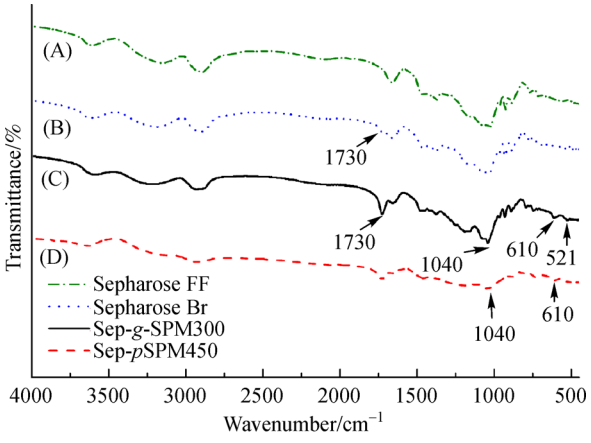

Fig. 1 FTIR spectra of (A) Sepharose FF, (B) Sepharose Br, (C) Sep-*g*-SPM300, and (D) Sep-*p*SPM450

1730 cm^{-1}, which is consistent with the result in previous works [6,11]. The stretching vibration of carbonyl group is more pronounced in representative Sep-*g*-SPM300 (Fig. 1(C)). It is attributed to the characteristic peak of C = O bond in methacrylate of grafted polymer. In Fig. 1(C), moreover, the peaks at 1040, 610 and 521 cm^{-1} of Sep-*g*-SPM300 represent stretching of sulfone groups. These characteristic peaks at 1040, 610 and 1730 cm^{-1} were also observed in Sep-*p*SPM450 (Fig. 1(D)). The FTIR spectra in Fig. 1 revealed the successful polymer grafting on Sep-*g*-SPM300 and Sep-*p*SPM450. IC and r_{pore} values of all the cation exchangers are also listed in Table 3. In this work, r_{pore} of all the gels was determined by iSEC experiments in a Tricorn 5/50 column (GE Healthcare, Uppsala, Sweden) at 50 and 200 $mmol \cdot L^{-1}$ NaCl. All the iSEC calibration curves for the gels are plotted in Fig. 2. It is clear that K_D values decrease with an increase of IC among the same cation exchangers. At the similar IC, Sep-*g*-SPM cation exchangers have larger K_D values for the dextran probe than Sep-*p*SPM cation exchangers. The result in Table 3 shows that r_{pore} of commercial Sepharose FF is 18.7 nm at 50 $mmol \cdot L^{-1}$ NaCl, which is consistent with the result reported in previous works [5,8]. With the introduction of polymer chains, r_{pore} of the cation exchangers decreases dramatically. In Sep-*g*-SPM cation exchangers, the grafting-from ATRP approach controllably introduces polymer chains with the regular distribution of the ligand [6,30]. As IC increases to 204 $mmol \cdot L^{-1}$, r_{pore} of Sep-*g*-SPM200 decreases to 15.7 nm. It is noteworthy in Table 3 that layer depths in Sep-*g*-SPM100 and Sep-*g*-SPM200 are 1.3 and 3.0 nm, respectively. Both the depths are smaller than the molecular size of lysozyme (50 × 30 Å) [11,31,32] and γ-globulin (235 × 44 × 44 Å) [32–34], indicating a monolayer adsorption of proteins on pore surfaces of Sep-*g*-SPM100 and Sep-*g*-SPM200. Among Sep-*g*-SPM cation exchangers in Table 3, there is a minimal value of r_{pore} in Sep-*g*-SPM300 while the layer depth of the cation exchanger increases to 9.1 nm. Thus, Sep-*g*-SPM300 provides structural basis for multilayer adsorption of proteins. At the similar IC, Sep-*p*SPM cation exchangers have smaller r_{pore} than Sep-*g*-SPM cation exchangers. For instance, r_{pore} of Sep-*p*SPM200 is smaller than that of Sep-*g*-SPM200 while the layer depth of Sep-*p*SPM200 is over twice higher than Sep-*g*-SPM200 due to the irregular chain distribution of polymer layer in Sep-*p*SPM cation exchangers. The result indicates that the grafting-to approach can bring about different architecture of polymer layer and ligand arrangement in the polymer-grafted cation exchangers compared with the grafting-from approach. Among Sep-*p*SPM cation exchangers in Table 3, there is a minimum value of r_{pore} in Sep-*p*SPM450. As the salt concentration increases to 200 $mmol \cdot L^{-1}$, r_{pore} of the polymer-grafted cation-exchangers increases obviously by 1.7%–9.1%, largely meaning partial shrinkage of polymer layer at 200 $mmol \cdot L^{-1}$ NaCl due to the shielding of electrostatic repulsion. It was also observed previously in our group [6,11] and the polymeric membrane reported by Luo and Wan [35]. Therefore, Sep-*g*-SPM and Sep-*p*SPM cation exchangers provide a platform to investigate the influence of grafting techniques and resulting architecture of polymer layer on protein adsorption.

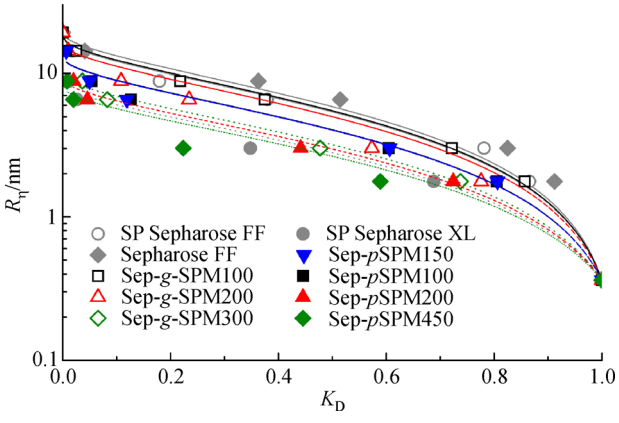

Fig. 2 Dextran calibration curves for Sepharose FF, SP Sepharose FF, SP Sepharose XL, Sep-*g*-SPM and Sep-*p*SPM cation exchangers. In the measurements, 50 $mmol \cdot L^{-1}$ NaCl in 20 $mmol \cdot L^{-1}$ Tris-HCl buffer (pH 8.0) was used as the liquid phase

3.2 Adsorption equilibria on polymer-grafted cation exchangers

Adsorption equilibria for lysozyme and γ-globulin on SP Sepharose FF, SP Sepharose XL, Sep-*g*-SPM and Sep-*p*SPM cation exchangers at 50 $mmol \cdot L^{-1}$ NaCl are shown in Fig. 3. As shown in Fig. 3(a), the adsorption density for lysozyme increases with IC. Langmuir parameters of protein adsorption on the cation exchangers, q_m and K_d, are summarized in Table 4. Among Sep-*g*-SPM cation exchangers, the maximal q_m for lysozyme is 363 $mg \cdot mL^{-1}$ in Sep-*g*-SPM300, which is comparable with the result

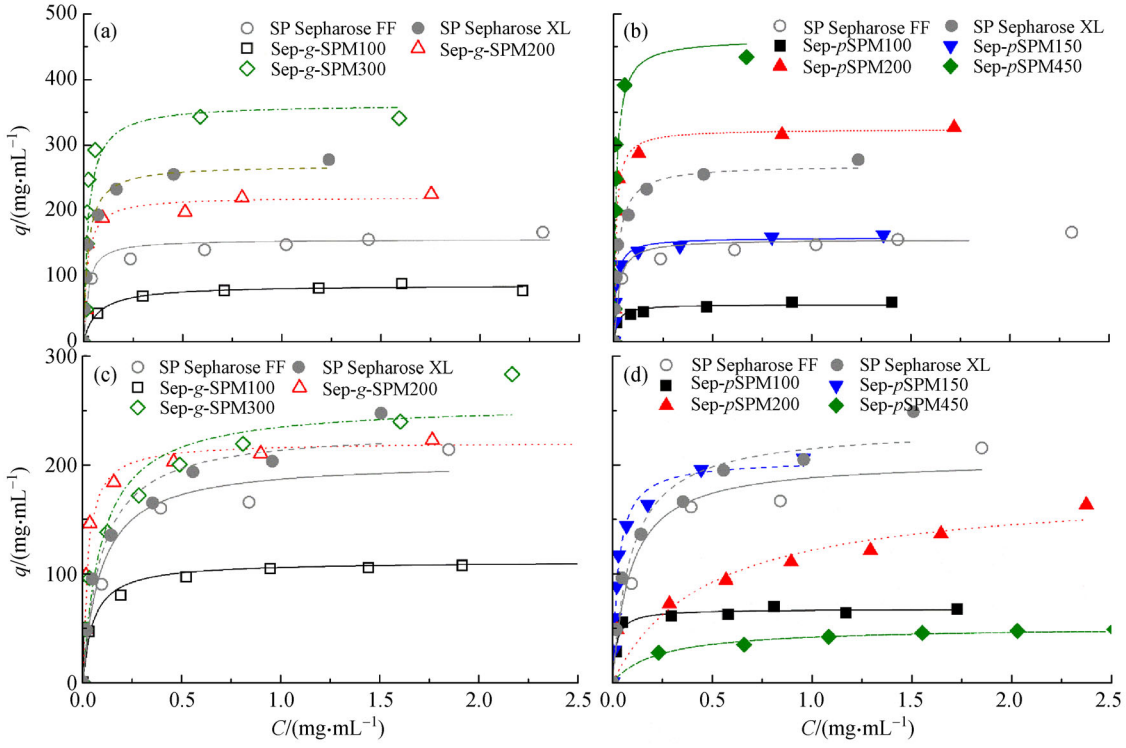

Fig. 3 Adsorption isotherms of lysozyme (a, b) and γ-globulin (c, d) on Sep-*g*-SPM (a, c) and Sep-*p*SPM (b, d) cation exchangers. Adsorption buffer is 50 mmol·L^{-1} NaCl in 20 mmol·L^{-1} Tris-HCl buffer (pH 8.0) for lysozyme adsorption and 50 mmol·L^{-1} NaCl in 20 mmol·L^{-1} acetate buffer (pH 4.5) for γ-globulin adsorption. The curves in the figure are the fitted Langmuir isotherm by Eq. (1)

previously reported in SPM polymer-grafted Sepharose FF at the similar ligand density [6] but much higher than those in Sep-*g*-SPM200 and SP Sepharose FF in Table 4. The latter is typical of monolayer lysozyme adsorption due to two-dimensional ligand distribution of SP Sepharose FF or a layer depth lower than the molecular size of lysozyme in Sep-*g*-SPM200. In contrast, a layer depth of 9.1 nm in Sep-*g*-SPM300 provides a 3-D ligand distribution and enough space for lysozyme adsorption, leading to a high adsorption capacity for lysozyme in Sep-*g*-SPM300. Among Sep-*p*SPM cation exchangers, adsorption density for lysozyme increases likely with IC as shown in Fig. 3(b), and the maximum q_m for lysozyme is 462 mg·mL^{-1} in Sep-*p*SPM450, which is close to the upper limit of lysozyme adsorption on Sepharose FF predicted by Zhang et al. [11], and by far the highest level of lysozyme adsorption capacity reported in Sepharose FF [11,18]. For Sep-*p*SPM cation exchangers, the relationship of q_m and IC in Fig. 4 shows that there is an IC around 150 mmol·L^{-1}, above which q_m for lysozyme increases greatly. This result is similar to BSA adsorption on PEI-grafted anionic exchangers reported by Yu et al. [8]. Moreover, the results in Table 4 show that there is no correlation between layer depth and q_m for lysozyme. Although Sep-*p*SPM100 has a larger layer depth than Sep-*g*-SPM200, the latter has a much higher q_m for lysozyme. On the other hand, Sep-*g*-SPM300 has a higher IC and q_m for lysozyme than Sep-*p*SPM200 even though both the cation exchangers have similar layer depths (listed in Table 3). The phenomenon was also observed in Sep-*p*SPM cation exchangers synthesized by the grafting-to approach. Sep-*p*SPM150 has a higher q_m for lysozyme than Sep-*p*SPM100 even though they have a similar layer depth (6.3 *vs.* 6.2 nm in Table 3). Our result of lysozyme adsorption demonstrated that IC is the dominant factor of q_m for lysozyme on polymer-grafted cation exchangers regardless of layer depth and grafting technique.

Adsorption equilibria of γ-globulin on Sep-*g*-SPM cation exchangers is presented in Fig. 3(c). Among Sep-*g*-SPM cation exchangers, adsorption density for γ-globulin increases with IC. In Table 4, the maximum q_m for γ-globulin is 256.9 mg·mL^{-1} in Sep-*g*-SPM300. It was likely attributed to multilayer adsorption on Sep-*g*-SPM300. The result of protein adsorption on Sep-*g*-SPM cation exchangers revealed that high-capacity adsorption of lysozyme and γ-globulin could be achieved simultaneously in Sep-*g*-SPM300 with spare chain density. The statement was also testified by Zhang et al. [11]. In contrast, adsorption capacity for γ-globulin decreases markedly with IC at a dense chain density as reported by Wang et al. [6], probably due to the repulsive interaction of the protein and polymer in a denser polymer chain [36].

Table 4 Langmuir parameters and D_e/D_0 for lysozyme and γ-globulin adsorption

Name	Lysozyme			γ-globulin		
	q_m/(mg·mL^{-1})	K_d/(mg·mL^{-1})	D_e/D_0	q_m/(mg·mL^{-1})	K_d/(mg·mL^{-1})	D_e/D_0
SP Sepharose FF	156.1±6.8	0.020±0.008	0.403	203.6±16.4	0.090±0.030	0.094
SP Sepharose XL	269.5±7.7	0.022±0.003	0.572	233.3±13.4	0.090±0.020	0.308
Sep-*g*-SPM100	86.3±2.3	0.072±0.013	0.391	111.2±3.2	0.050±0.010	0.363
Sep-*g*-SPM200	220.5±15.7	0.019±0.006	0.602	221.1±6.2	0.024±0.003	0.077
Sep-*g*-SPM300	362.9±33.9	0.023±0.007	0.130	256.9±15.8	0.090±0.030	0.033
Sep-*p*SPM100	56.5±2.8	0.019±0.007	0.170	66.8±1.9	0.019±0.004	0.100
Sep-*p*SPM150	158.8±5.1	0.013±0.002	0.181	203.3±6.0	0.027±0.003	0.033
Sep-*p*SPM200	324.3±18.6	0.010±0.002	0.114	177.7±28.3	0.471±0.244	0.088
Sep-*p*SPM450	462.4±50.3	0.012±0.004	0.051	50.7±1.6	0.233±0.041	0.099

For Sep-*p*SPM cation exchangers, γ-globulin adsorption in Fig. 3(d) exhibits distinct characteristics in lysozyme adsorption and the maximal q_m for γ-globulin was obtained in Sep-*p*SPM150. As IC increases to 455 mmol·L^{-1}, q_m for γ-globulin decreases to 50.7 mg·mL^{-1}, whereas layer depths increase to 10.9 nm. The larger layer depth is, the stronger repulsive interaction is. This suggests that γ-globulin adsorption on Sep-*p*SPM cation exchangers is not related to IC, but dependent on the repulsive interaction of polymer layer as stated previously in our group [6,11]. Further comparison of γ-globulin adsorption on Sep-*g*-SPM and Sep-*p*SPM cation exchangers in Table 4 shows that Sep-*p*SPM200 has a smaller q_m for γ-globulin than Sep-*g*-SPM300 even though both the cation exchangers have similar layer depths. This indicates that the grafting-to approach can bring about more serious repulsive interaction than the grafting-from approach at the same layer depth due to there was irregular chain distribution of polymer layer in Sep-*p*SPM cation exchangers. Table 4 also shows that SP Sepharose XL and Sep-*p*SPM450 of the similar layer depths likely have enormous difference in q_m for γ-globulin, implying that *p*SPM layer in Sep-*p*SPM450 can bring about more serious repulsive interaction to γ-globulin than dextran layer in SP Sepharose XL. Therefore, grafting techniques and the resulting architecture of polymer layer have a significant influence to γ-globulin adsorption.

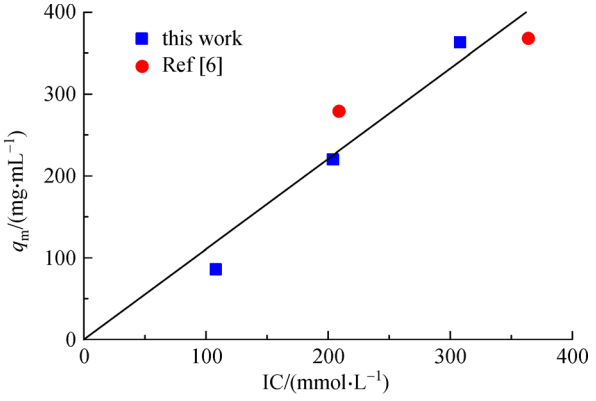

Fig. 4 q_m for lysozyme on Sep-*p*SPM cation exchangers as a function of ionic capacity. The symbol solid square (■) stands for q_m for lysozyme on Sep-*p*SPM cation exchangers, and solid circle (●) for q_m for lysozyme in [6]. The straight line was obtained by fitting with all the experimental data

3.3 Influence of salt concentration on protein adsorption

Protein adsorption was further investigated in Sep-*g*-SPM300 and Sep-*p*SPM450 at various salt concentrations. The result is shown in Fig. 5. For lysozyme adsorption in Figs. 5(a,b), adsorption densities of Sep-*g*-SPM300 and Sep-*p*SPM450 decrease markedly at 100 mmol·L^{-1} NaCl and over, a typical characteristic of protein adsorption on ionic exchangers. At 200 mmol·L^{-1} NaCl, q_m for lysozyme decreases by about 40% in Sep-*g*-SPM300 and 16% in Sep-*p*SPM450 compared with their extreme values of q_m in Table 5. In the same range, q_m for lysozyme of SP Sepharose FF decreases significantly by 62% as reported by Wang et al. [6]. In this work, a smaller drop of q_m for lysozyme with salt concentration could be attributed to the presence of polymer layer in Sep-*g*-SPM300 and Sep-*p*SPM450. As salt concentration increases from 50 to 200 mmol·L^{-1}, the layer depths decreases by 6.6% in Sep-*g*-SPM300 and less by 5.1% in Sep-*p*SPM450 (Table 3), meaning a slight shrinkage of polymer layer. Hence, Sep-*g*-SPM300 and Sep-*p*SPM450 still provide three-dimensional ligand distribution and enough space for protein adsorption at 200 mmol·L^{-1} NaCl. On the other hand, high values of K_d were obtained at 200 mmol·L^{-1} NaCl in Table 5 because electrostatic interaction between protein and ion-exchange ligand decreases with an increase of salt concentration.

For γ-globulin adsorption, salt concentration distinctly affects γ-globulin adsorption on Sep-*g*-SPM300 and Sep-*p*SPM450, as shown in Figs. 5(c,d). Sep-*g*-SPM300 has much higher adsorption densities than Sep-*p*SPM450 and

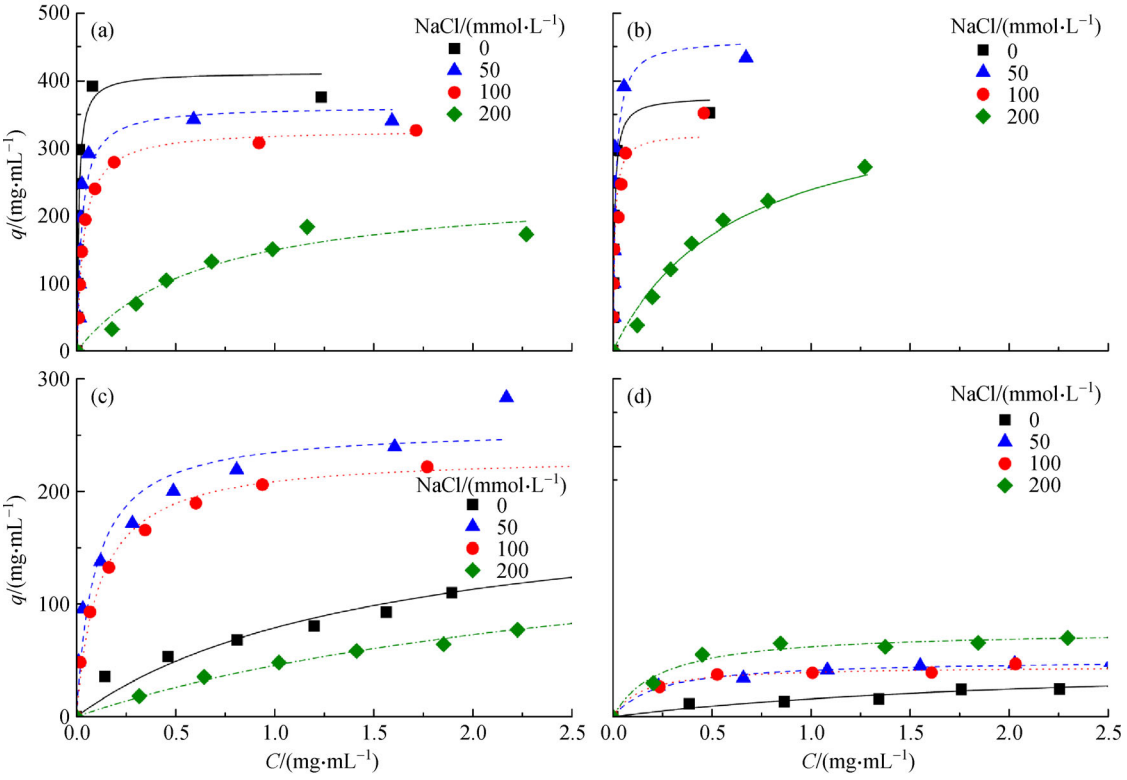

Fig. 5 Adsorption isotherms of (a,b) lysozyme and (c,d) γ-globulin on (a,c) Sep-*g*-SPM300 and (b,d) Sep-*p*SPM450 at various salt concentrations. In the experiments, the base adsorption buffers are the same as those in Fig. 3 and salt concentrations of 0, 50, 100 and 200 mmol·L^{-1} were adjusted by adding NaCl

Table 5 Langmuir parameters and $D_e/D0$ for lysozyme and γ-globulin adsorption at various salt concentrations

Name	Proteins		C_{NaCl}/(mmol·L^{-1})			
			0	50	100	200
Sep-*g*-SPM300	Lysozyme	q_m/(mg·mL^{-1})	412.7±37.7	362.9±33.9	328.3±7.3	246.5±32.1
		K_d/(mg·mL^{-1})	0.009±0.002	0.023±0.007	0.033±0.003	0.645±0.203
		D_e/D_0	0.090	0.130	0.301	0.542
	γ-Globulin	q_m/(mg·mL^{-1})	200.1±23.7	256.9±15.8	233.0±5.6	182.5±12.5
		K_d/(mg·mL^{-1})	1.54±0.40	0.09±0.03	0.12±0.01	3.02±0.37
		D_e/D_0	0.077	0.033	0.088	1.100
Sep-*p*SPM450	Lysozyme	q_m/(mg·mL^{-1})	377.3±44.4	462.4±50.3	322.5±24.1	387.5±27.5
		K_d/(mg·mL^{-1})	0.008±0.002	0.012±0.004	0.008±0.003	0.626±0.103
		D_e/D_0	0.059	0.051	0.108	0.481
	γ-Globulin	q_m/(mg·mL^{-1})	51.4±8.3	50.7±1.6	45.1±1.8	77.1±2.9
		K_d/(mg·mL^{-1})	2.24±0.74	0.233±0.041	0.148±0.040	0.244±0.048
		D_e/D_0	–	0.099	0.231	0.198

the maximal adsorption density of Sep-*g*-SPM300 was observed at 50 mmol·L^{-1} NaCl. Langmuir parameters in Table 5 further show that q_m for γ-globulin on Sep-*g*-SPM300 changes from 182.5 to 256.9 mg·mL^{-1} in salt concentration range of 0–200 mmol·L^{-1} NaCl, indicating that the influence of salt concentration is limited in γ-globulin adsorption on Sep-*g*-SPM300 due to the presence of rather stable polymer layer. It is much higher than q_m for γ-globulin on Sep-*p*SPM450 gel (45.1–77.1 mg·mL^{-1} in Table 5). From protein adsorption on Sep-*g*-SPM and Sep-*p*SPM cation exchangers in this work, it could be concluded that the grafting-from approach is

more beneficial for high-capacity adsorption of proteins because it always brings about regular ligand distribution and less repulsive interaction.

3.4 Adsorption kinetics of lysozyme and γ-globulin

The trajectories of lysozyme and γ-globulin uptake onto the cation exchangers are shown in Fig. 6. For SP Sepharose FF and SP Sepharose XL, liquid phase concentration of lysozyme decreases rapidly in the initial 30 min and uptake curves of lysozyme can well be predicted by pore diffusion model in Eqs. (2–4). As listed in Table 4, D_e/D_0 for lysozyme are 0.403 in SP Sepharose FF and 0.572 in SP Sepharose XL. D_0 is protein diffusivity in free solution. Intraparticle mass transfer of lysozyme in SP Sepharose FF is typical of pore size dependent hindered diffusion. In Fig. 6(a), Sep-*g*-SPM100 exhibits similar trajectory of lysozyme uptake to commercial cation exchangers, and liquid phase protein concentration decreases rapidly in the initial stages. In Table 4, D_e/D_0 for lysozyme is 0.391 in Sep-*g*-SPM100, which is close to that in SP Sepharose FF, affirming that the influence of polymer layer in Sep-*g*-SPM100 could be ignored because its layer depth is lower than molecular size of lysozyme. Furthermore, D_e/D_0 values of Sep-*g*-SPM200 are higher than that reported by Wang et al. at the same IC [6] probably due to more spare chain density of Sep-*g*-SPM cation exchangers and resulting larger pore size (expressed as r_{pore}) in Sep-*g*-SPM200. A further shrinkage of pore size leads to a slower decrease of liquid phase protein concentration during lysozyme uptake of Sep-*g*-SPM300 (Fig. 6(a)). For Sep-*p*SPM cation exchangers, liquid phase lysozyme concentration decreases rapidly in Sep-*p*SPM100 and Sep-*p*SPM150. With an increase of IC, liquid phase lysozyme concentration decreases more slowly (Fig. 6(b)). Accordingly, D_e/D_0 values decrease to 0.051 in Sep-*p*SPM450 gel (Table 4). A comparison of D_e/D_0 and r_{pore} further indicates that there are similar D_e/D_0 values between Sep-*p*SPM100 and Sep-*p*SPM150 with the similar pore sizes (listed in Table 3). The conclusion is also claimed between Sep-*p*SPM200 and Sep-*g*-SPM300 even though they were prepared via different grafting techniques. Therefore, lysozyme uptake rate in polymer-grafted cation exchangers depends on pore sizes regardless of grafting technique.

The trajectories of γ-globulin uptake on Sep-*g*-SPM cation exchangers are presented in Fig. 6(c). The result shows that liquid phase protein concentration also decreases with contact time during γ-globulin uptake on commercial cation exchangers. As shown in Table 4, D_e/D_0 for γ-globulin is 0.094 in SP Sepharose FF and 0.308 in SP Sepharose XL. The similar trajectory was also observed in γ-globulin uptake on Sep-*g*-SPM cation exchangers. By fitting with pore diffusion model, D_e/D_0 for γ-globulin is 0.363 in Sep-*g*-SPM100 as listed in Table 4. With an increase of IC, D_e/D_0 values for γ-globulin decrease to

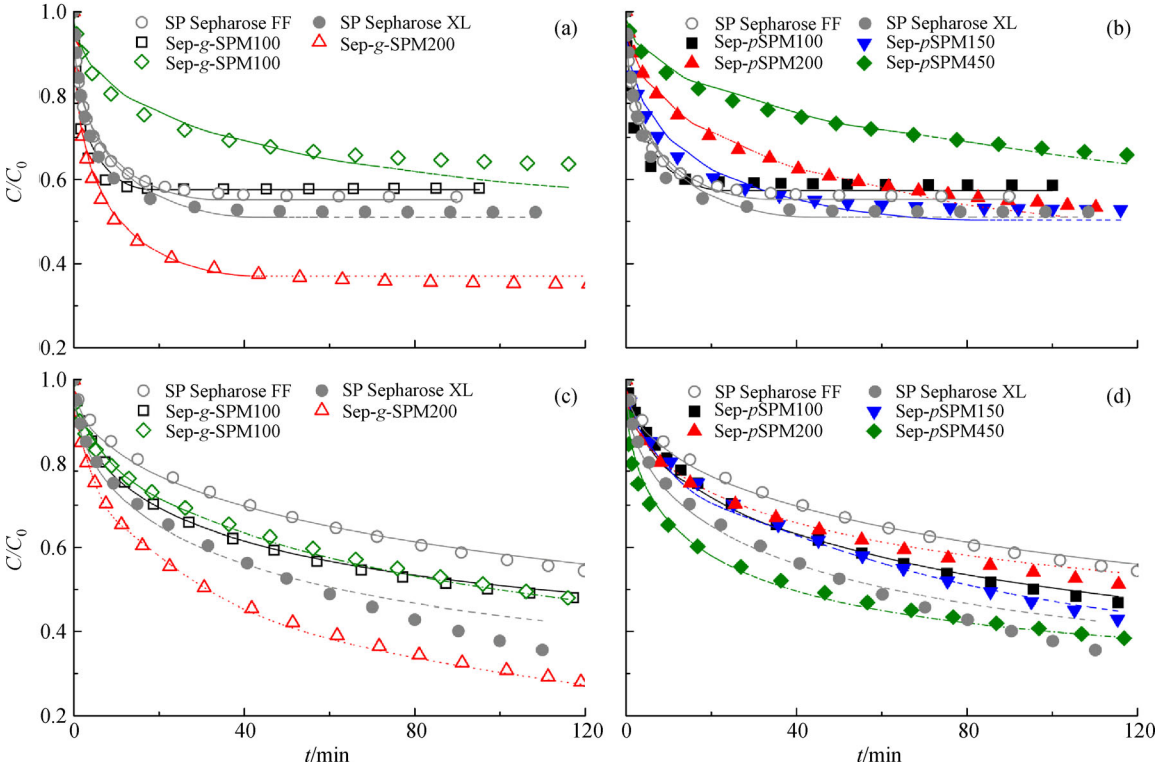

Fig. 6 Uptake curves of (a, b) lysozyme and (c, d) γ-globulin on (a, c) Sep-*g*-SPM and (b, d) Sep-*p*SPM cation exchangers. The buffers are the same as those in Fig. 3

0.033 in Sep-*g*-SPM300 while r_{pore} decreases to 9.6 nm. This trend is consistent with that reported by Wang et al. [6]. Compared with Sep-*g*-SPM cation exchangers, Sep-*p*SPM150 gel has a minimal D_e/D_0 for γ-globulin among Sep-*p*SPM gels. With a further increase of IC, D_e/D_0 increase by 167% in Sep-*p*SPM200 and by 200% in Sep-*p*SPM450. It is probably a "chain delivery" effect as described by Yu et al. [8] to result in an increase of D_e/D_0 for γ-globulin at IC larger than 150 mmol·L^{-1}. The result in this work suggests that the facilitated transport of adsorbed γ-globulin could occur only in Sep-*p*SPM cation exchangers. In Sep-*g*-SPM cation exchangers, a low chain density leads to spare distribution of polymer chain and the adjacent polymers are too far from each other to deliver adsorbed γ-globulin. Therefore, the architecture of polymer layers has a significant influence on intraparticle mass transfer of γ-globulin. Although Sep-*p*SPM200 and Sep-*g*-SPM300 synthesized via different grafting techniques have a similar r_{pore}, facilitated transport of adsorbed γ-globulin leads to a 1.6-times higher D_e/D_0 for γ-globulin in Sep-*p*SPM200 than in Sep-*g*-SPM300. The influence of the architecture of polymer layers was also observed in Sep-*p*SPM450 and SP Sepharose XL. Although Sep-*p*SPM450 and SP Sepharose XL have a similar r_{pore}, Sep-*p*SPM450 has a much lower D_e/D_0 for γ-globulin than SP Sepharose XL, indicating that facilitated transport of adsorbed γ-globulin is more significant in SP Sepharose XL. This suggests that dextran layer and *p*SPM layer lead to different contribution in facilitating γ-globulin uptake rate. Uptake results in this work further confirmed that the grafting techniques and the thus resulting architecture of polymer layers have a distinct influence in protein uptake and the facilitated transport of γ-globulin only occurs in Sep-*p*SPM cation exchangers synthesized via the grafting-to approach.

3.5 Influence of salt concentration on protein uptake

Lysozyme and γ-globulin uptakes of Sep-*g*-SPM300 and Sep-*p*SPM450 were further investigated at various salt concentrations. The result is presented in Fig. 7. Figure 7(a) shows that with an increase of salt concentration during lysozyme uptake in Sep-*g*-SPM300, liquid phase protein concentration decreases at a faster rate, and approaches an equilibrium after 30 min at 200 mmol·L^{-1} NaCl. For lysozyme uptake in Sep-*p*SPM450 (Fig. 7 (b)), however, liquid phase protein concentration decreases slower at the same salt concentration. Accordingly, Sep-*g*-SPM300 has a higher D_e/D_0 for lysozyme than Sep-*p*SPM450 at the same salt concentrations below 200 mmol·L^{-1} NaCl (Table 5); at 100 mmol·L^{-1} NaCl, D_e/D_0 of Sep-*g*-SPM300 is 179% higher than that of Sep-*p*SPM450. This is consistent with the result in Table 3 that Sep-*g*-SPM300 has a larger r_{pore} than Sep-*p*SPM450. γ-Globulin

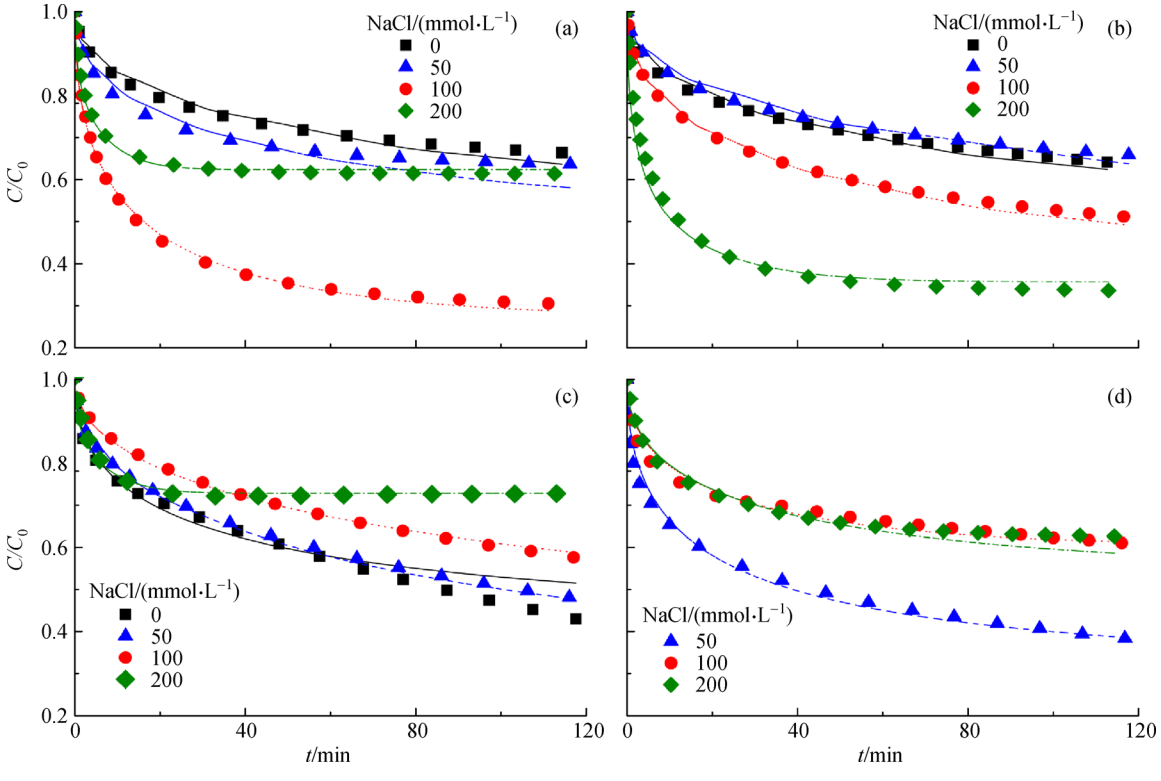

Fig. 7 Uptake of (a, b) lysozyme and (c, d) γ-globulin on (a, c) Sep-*g*-SPM300 and (b, d) Sep-*p*SPM450 at various salt concentrations. In the measurements, the adsorption buffers are the same as those in Fig. 3 and salt concentrations of 0, 50, 100 and 200 mmol·L^{-1} were adjusted by adding NaCl

uptakes in Sep-*g*-SPM300 and Sep-*p*SPM450 are presented in Figs. 7(c, d). The result shows that liquid phase concentration of γ-globulin decreases at a faster rate in Sep-*p*SPM450 at NaCl concentrations below 200 mmol·L^{-1}. As listed in Table 5, therefore, higher D_e/D_0 values for γ-globulin are obtained in Sep-*p*SPM450 gels at 50 and 100 mmol·L^{-1} NaCl. The result is in contrast with lysozyme uptakes shown in Figs. 7(a, b), suggesting that intraparticle mass transfer of γ-globulin is not dependent on r_{pore}. Therefore, the results in Figs. 7(c, d) provide indirect evidence that intraparticle mass transfer of γ-globulin is influenced by the architecture of polymer layers, and is more beneficial from Sep-*p*SPM cation exchangers prepared via the grafting-to approach.

3.6 Dynamic binding capacities

DBCs for lysozyme and γ-globulin on Sep-*g*-SPM300 and Sep-*p*SPM450 cation exchangers at 50 mmol·L^{-1} NaCl are listed in Table 6. As shown in Table 6, both the cation exchangers have high DBCs for lysozyme and DBC in Sep-*g*-SPM300 reaches 190 mg·mL^{-1} which is equivalent to the DBC results reported previously in our group [6,11]. The ratio of DBC to q_m is also listed in Table 6. At a flow rate of 1.0 mL·min^{-1}, DBC/q_m of Sep-*g*-SPM300 is 0.52, indicating a high availability of the cation exchanger. Meanwhile, DBC/q_m of Sep-*p*SPM450 is 0.24 even though Sep-*p*SPM450 has a much higher q_m than Sep-*g*-SPM300, possibly due to 1.55-times higher D_e/D_0 for lysozyme of Sep-*g*-SPM300 than that of Sep-*p*SPM450 as listed in Table 5. As listed in Table 6, however, DBC for γ-globulin is 33 mg·mL^{-1} in Sep-*g*-SPM300 and only 5 mg·mL^{-1} in Sep-*p*SPM450. In this case, higher D_e/D_0 for γ-globulin in Sep-*p*SPM450 also plays an important role. However, a much lower q_m for γ-globulin in Sep-*p*SPM450 means the limited availability of the cation exchangers in chromatographic performance. Unlike DBC/q_m values for lysozyme, both the cation exchangers have similar DBC/q_m values for γ-globulin. The DBC result further demonstrated the role of adsorption capacity and intraparticle mass transfer in polymer-grafted cation exchangers.

4 Conclusions

In conclusion, we have synthesized Sep-*g*-SPM and Sep-*p*SPM cation exchangers via grafting-from and grafting-to approaches, respectively, and investigated the role of grafting techniques on the performance of protein adsorption. The results show that polymer layers on pore surfaces of the cation exchangers provide a stable three-dimensional ligand distribution and spaces for protein adsorption. At the same ligand densities, Sep-*g*-SPM can controllably introduce polymer chains with the regular distribution of the ligand, and thus has larger r_{pore} and smaller layer depths of polymer than Sep-*p*SPM. Therefore, high-capacity adsorption of lysozyme and γ-globulin could be achieved simultaneously in Sep-*g*-SPM300. However, Sep-*p*SPM has an irregular chain distribution of polymer layer and different architecture of polymer layers from Sep-*g*-SPM cation exchangers. This leads to more serious repulsive interaction to γ-globulin, and thus a lower adsorption capacity for γ-globulin in Sep-*p*SPM with the similar IC to Sep-*g*-SPM. Moreover, the result of protein uptakes shows that the facilitated transport of adsorbed γ-globulin occurs only in Sep-*p*SPM and depends on the architecture of polymer layers. This work provides insight into the role of grafting techniques in protein adsorption on polymer-grafted ion exchangers, and a clear clue for the development of high-performance protein chromatography.

Acknowledgements This work was supported by grants from the National Natural Science Foundation of China (Grant Nos. 21476166 and 21236005), the Open Funding Project of the State Key Laboratory of Biochemical Engineering (No. 2014KF-03) and the Tianjin Natural Science Foundation (15JCYBJC48500).

References

1. Savina I NGalaev I Y, Mattiasson B. Ion-exchange macroporous hydrophilic gel monolith with grafted polymer brushes. Journal of Molecular Recognition, 2006, 19(4): 313–321
2. Perez-Almodovari E X, Wu Y, Carta G. Multicomponent adsorption of monoclonal antibodies on macroporous and polymer grafted cation exchangers. Journal of Chromatography A, 2012, 1264: 48–56
3. Basconi J E, Carta G, Shirts M R. Multiscale modeling of protein adsorption and transport in macroporous and polymer-grafted ion exchangers. AIChE Journal. American Institute of Chemical Engineers, 2014, 60(11): 3888–3901
4. Lenhoff A M. Protein adsorption and transport in polymer-functionalized ion-exchangers. Journal of Chromatography A, 2011, 1218(49): 8748–8759
5. Stone M C, Carta G. Protein adsorption and transport in agarose and dextran-grafted agarose media for ion exchange chromatography. Journal of Chromatography A, 2007, 1146(2): 202–215
6. Wang H Y, Sun Y, Zhang S L, Luo J, Shi Q H. Fabrication of high-

Table 6 DBCs of Sep-*g*-SPM300 and Sep-*p*SPM450 cation exchangers

Name	Lysozyme		γ-globulin	
	DBC/(mg·mL^{-1})	DBC/q_m	DBC/(mg·mL^{-1})	DBC/q_m
Sep-*g*-SPM300	190±2	0.52	33±3	0.13
Sep-*p*SPM450	111±2	0.24	5±1	0.10

capacity cation-exchangers for protein chromatography by atom transfer radical polymerization. Biochemical Engineering Journal, 2016, 113: 19–29

7. Bowes B D, Koku H, Czymmek K J, Lenhoff A M. Protein adsorption and transport in dextran-modified ion-exchange media. I: Adsorption. Journal of Chromatography A, 2009, 1216(45): 7774–7784
8. Yu L L, Tao S P, Dong X Y, Sun Y. Protein adsorption to poly (ethylenimine)-modified Sepharose FF: I. A critical ionic capacity for drastically enhanced capacity and uptake kinetics. Journal of Chromatography A, 2013, 1305: 76–84
9. Shi Q H, Jia G D, Sun Y. Dextran-grafted cation exchanger based on superporous agarose gel: Adsorption isotherms, uptake kinetics and dynamic protein adsorption performance. Journal of Chromatography A, 2010, 1217(31): 5084–5091
10. Tao Y, Carta G, Ferreira G, Robbins D. Adsorption of deamidated antibody variants on macroporous and dextran-grafted cation exchangers: I. Adsorption equilibrium. Journal of Chromatography A, 2011, 1218(11): 1519–1529
11. Zhang S L, Zhao M, Yang W, Luo J, Sun Y, Shi Q H. A novel polymer-grafted cation exchanger for high-capacity protein chromatography: The role of polymer architecture. Biochemical Engineering Journal, 2017, 128: 218–227
12. Unsal E, Elmas B, Caglayan B, Tuncel M, Patir S, Tuncel A. Preparation of an ion-exchange chromatographic support by a "grafting from" strategy based on atom transfer radical polymerization. Analytical Chemistry, 2006, 78(16): 5868–5875
13. Yu L L, Sun Y. Protein adsorption to poly(ethylenimine)-modified Sepharose FF: II. Effect of ionic strength. Journal of Chromatography A, 2013, 1305: 85–93
14. Chang C, Lenhoff A M. Comparison of protein adsorption isotherms and uptake rates in preparative cation-exchange materials. Journal of Chromatography A, 1998, 827(2): 281–293
15. Staby A, Jensen I H, Mollerup I. Comparison of chromatographic ion-exchange resins I. Strong anion-exchange resins. Journal of Chromatography A, 2000, 897(1-2): 99–111
16. Bowes B D, Lenhoff A M. Protein adsorption and transport in dextran-modified ion-exchange media. II. Intraparticle uptake and column breakthrough. Journal of Chromatography A, 2011, 1218 (29): 4698–4708
17. Bowes B D, Lenhoff A M. Protein adsorption and transport in dextran-modified ion-exchange media. III. Effects of resin charge density and dextran content on adsorption and intraparticle uptake. Journal of Chromatography A, 2011, 1218(40): 7180–7188
18. Ubiera A R, Carta G. Radiotracer measurements of protein mass transfer: Kinetics in ion exchange media. Biotechnology Journal, 2006, 1(6): 665–674
19. Dismer F, Petzold M, Hubbuch J. Effects of ionic strength and mobile phase pH on the binding orientation of lysozyme on different ion-exchange adsorbents. Journal of Chromatography A, 2008, 1194(1): 11–21
20. Hubbuch J, Linden T, Knieps E, Ljunglof A, Thommes J, Kula M R. Mechanism and kinetics of protein transport in chromatographic media studied by confocal laser scanning microscopy. Part I. The interplay of sorbent structure and fluid phase conditions. Journal of Chromatography A, 2003, 1021(1-2): 93–104
21. Chan J W, Huang A, Uhrich K E. Self-assembled amphiphilic macromolecule coatings: Comparison of grafting-from and grafting-to approaches for bioactive delivery. Langmuir, 2016, 32(20): 5038–5047
22. Reznik C, Landes C F. Transport in supported polyelectrolyte brushes. Accounts of Chemical Research, 2012, 45(11): 1927–1935
23. Hansson S, Trouillet V, Tischer T, Goldmann A S, Carlmark A, Barner-Kowollik C, Malmstrom E. Grafting efficiency of synthetic polymers onto biomaterials: A comparative study of grafting-from *versus* grafting-to. Biomacromolecules, 2013, 14(1): 64–74
24. Minko S. Grafting on solid surfaces: "Grafting to" and "grafting from" methods. In: Stamm M, ed. Polymer Surfaces and Interfaces: Characterization, Modification and Applications. Berlin: Springer Berlin Heidelberg, 2008, 215–234
25. Wang Z G, Wan L S, Xu Z K. Surface engineerings of polyacrylonitrile-based asymmetric membranes towards biomedical applications: An overview. Journal of Membrane Science, 2007, 304(1-2): 8–23
26. Yu L L, Shi Q H, Sun Y. Effect of dextran layer on protein uptake to dextran-grafted adsorbents for ion-exchange and mixed-mode chromatography. Journal of Separation Science, 2011, 34(21): 2950–2959
27. Shi Q H, Zhou X, Sun Y. A novel superporous agarose medium for high-speed protein chromatography. Biotechnology and Bioengineering, 2005, 92(5): 643–651
28. Weaver L E, Carta G. Protein adsorption on cation exchangers: Comparison of macroporous and gel-composite media. Biotechnology Progress, 1996, 12(3): 342–355
29. Dephillips P, Lenhoff A M. Pore size distributions of cation-exchange adsorbents determined by inverse size-exclusion chromatography. Journal of Chromatography A, 2000, 883(1-2): 39–54
30. Li Q, Imbrogno J, Belfort G, Wang X L. Making polymeric membranes antifouling via "grafting from" polymerization of zwitterions. Journal of Applied Polymer Science, 2015, 132(21): n/a
31. Dismer F, Hubbuch J. A novel approach to characterize the binding orientation of lysozyme on ion-exchange resins. Journal of Chromatography A, 2007, 1149(2): 312–320
32. Koshari S H S, Wagner N J, Lenhoff A M. Effects of resin architecture and protein size on nanoscale protein distribution in ion-exchange media. Langmuir, 2018, 34(2): 673–684
33. Yang H, Gurgel P V, Carbonell R G. Purification of human immunoglobulin G via Fc-specific small peptide ligand affinity chromatography. Journal of Chromatography A, 2009, 1216(6): 910–918
34. Fair B D, Jamieson A M. Studies of protein adsorption on polystyrene latex surfaces. Journal of Colloid and Interface Science, 1980, 77(2): 525–534
35. Luo J, Wan Y. Effect of highly concentrated salt on retention of organic solutes by nanofiltration polymeric membranes. Journal of Membrane Science, 2011, 372(1-2): 145–153
36. CYoshikawa A, Goto Y, Tsujii T, Fukuda T, Kimura K, Yamamoto A, Kishida. Protein repellency of well-defined, concentrated poly(2-hydroxyethyl methacrylate) brushes by the size-exclusion effect. Macromolecules, 2006, 39(6): 2284–2290